PHYSICAL REVIEW E **87**, 030802(R) (2013)

Magnetic resonance pore imaging, a tool for porous media research

Stefan Hertel,[1] Mark Hunter,[1,2] and Petrik Galvosas[1,*]

[1]*MacDiarmid Institute for Advanced Materials and Nanotechnology, School of Chemical and Physical Sciences, Victoria University of Wellington, Wellington 6140, New Zealand*

[2]*Magritek Limited, 32 Salamanca Road, Wellington 6012, New Zealand*

(Received 20 October 2012; published 12 March 2013)

The internal structure of porous materials is of importance in many areas such as medicine, chemical engineering, and petrophysics. While diffraction methods such as x ray are widely used to study the internal pore space, these methods suffer from the loss of the phase information in the detected signals. Recently, an advanced diffusive diffraction NMR method was proposed [F. B. Laun *et al.*, Phys. Rev. Lett. **107**, 048102 (2011).] which is predicted to preserve the phase information, thus overcoming this severe limitation of diffraction methods in general. Here we provide experimental confirmation that the suggested approach is indeed able to acquire the diffractive signal including its phase which allows the direct image reconstruction of the pore space, averaged over all pores. We furthermore prove that this approach may combine the advantages of magnetic resonance imaging, namely, its robust and straightforward image reconstruction via a Fourier transformation with the much improved spatial resolution of pulsed gradient spin echo NMR.

DOI: 10.1103/PhysRevE.87.030802 PACS number(s): 91.60.−x, 61.43.Gt, 76.60.Pc, 82.56.Lz

Diffraction methods, such as x ray [1], neutron scattering [2], and pulsed gradient spin echo (PGSE)-NMR [3], are established tools for characterizing ordered and disordered porous materials. These techniques are able to obtain properties of the structure factor, a function which concisely describes the material in the Fourier space [1]. It is conventional wisdom that only the modulus of the structure factor can be measured [1,3], which prevents one from obtaining images by a simple inversion of acquired data. Recent advances of NMR based diffraction methods appear to lift this severe limitation. A general approach suggested by Laun *et al.* predicts that a modification of a single PGSE-NMR experiment is sufficient to acquire structure factors for arbitrary geometries [4]. Shemesh *et al.*, on the other hand, introduced a synergistic approach using two PGSE experiments [5]. It enables one to obtain the full structure factor for certain pore symmetries [6]. Here we provide experimental confirmation that the full structure factor and averaged pore images can indeed be acquired with a single PGSE experiment, as suggested by Laun *et al.* [4]. This led us to the design of a hybrid between magnetic resonance imaging (MRI) [7,8] and PGSE-NMR diffraction [3], which we call magnetic resonance pore imaging (MRPI). It combines the advantages of both methods, namely, direct imaging, inherited from MRI, with the high resolution of PGSE-NMR. Thus, in the context of porous media research, MRPI is able to provide information about the pores which is of particular importance when their shape determines the global properties of the material.

The method is an improvement of the "diffusive-diffraction" PGSE-NMR experiment [3] which comprises two magnetic field gradients and two radio frequency (RF) pulses. While the RF pulses create and refocus coherence of the nuclear spins, the gradients (of width δ and magnitude G) label spins with a spatially dependent phase. This phase is quantified by a scattering vector $\boldsymbol{q} = (2\pi)^{-1}\gamma\delta\boldsymbol{G}$ [9], with γ being the gyromagnetic ratio. If spin-bearing molecules remain at the same position all the time, the effect of the two gradients will compensate each other. However, if diffusing molecules are allowed to sample the voids in a porous system for a sufficiently long time in between the two gradients, diffraction-like patterns may be observed [3]. In the limit of an infinitely long gradient separation time and closed pores, the obtained NMR signal can be expressed as (see Ref. [10])

$$E_\infty(\boldsymbol{q}) = \int \rho(\boldsymbol{r}) \exp\{i2\pi\boldsymbol{q}\cdot\boldsymbol{r}\} d\boldsymbol{r} \int \rho(\boldsymbol{r}') \exp\{-i2\pi\boldsymbol{q}\cdot\boldsymbol{r}'\} d\boldsymbol{r}' = S_0^*(\boldsymbol{q}) S_0(\boldsymbol{q}) = |S_0(\boldsymbol{q})|^2. \quad (1)$$

$S_0(\boldsymbol{q})$ is the structure factor which contains all information about the spin density $\rho(\boldsymbol{r})$ but in a space reciprocal to real space [1]. If the voids of a porous material are filled with a fluid which gives rise to a detectable signal, then its density function $\rho(\boldsymbol{r})$ holds the information about the pore geometry. It is therefore highly desirable to measure $S_0(\boldsymbol{q})$ as it would directly return $\rho(\boldsymbol{r})$ upon Fourier transformation. Unfortunately, the inverse Fourier transformation of the signal $E_\infty(\boldsymbol{q})$ will not return $\rho(\boldsymbol{r})$ since the diffusive-diffraction PGSE-NMR experiment is unable to measure $S_0(\boldsymbol{q})$, only its squared modulus. This loss of the phase information is one of the similarities diffusive-diffraction PGSE-NMR experiments share with other diffraction methods and is commonly referred to as the "phase problem" [1].

To prevent the loss of phase information in PGSE-NMR, a minimal but ingenious modification of the experiment was suggested by Laun *et al.* [4] which extends one of the two gradient pulses to length δ_L, with reduced amplitude as shown in Fig. 1(a). If this pulse scheme, also referred to as long-narrow PGSE-NMR [11], is used for samples which consist of closed pores, the elongation of the first gradient pulse will lead to a successive phase accumulation over time depending on the trace of the molecules within the pore. At any given time the phase of a single molecule may be expressed by its averaged position up to this time. Since the molecules undergo restricted Brownian motion, their average positions for long

*petrik.galvosas@vuw.ac.nz

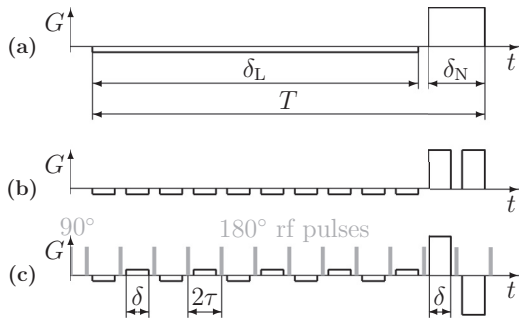

FIG. 1. Effective gradient scheme of the experiment as suggested by Laun *et al*. [4] (a) and its replacement used for this work (b). The actual applied gradients were alternating, interspersed with RF pulses (c). This results in a CPMG-like pulse sequence with a leading 90° excitation pulse followed by a train of 180° pulses. Gradients are in fact trapezoidal with a width of $\delta = 3.045$ ms (including ramp times). Note that the schemes are not to scale and many more pulses replacing the long gradient have been used than shown.

enough times will coincide with the position of the center of mass of the pore ($\boldsymbol{r}_{\mathrm{cm}}$), which allows Eq. (1) to be rewritten (in the limit of $\delta_L \to \infty$) as

$$E_\infty(\boldsymbol{q}) \propto \exp\{i2\pi\boldsymbol{q}\cdot\boldsymbol{r}_{\mathrm{cm}}\}\int \rho(\boldsymbol{r}')\exp\{-i2\pi\boldsymbol{q}\cdot\boldsymbol{r}'\}d\boldsymbol{r}'$$
$$\propto \exp\{i2\pi\boldsymbol{q}\cdot\boldsymbol{r}_{\mathrm{cm}}\}S_0(\boldsymbol{q}). \quad (2)$$

When comparing this result with corresponding expressions known from magnetic resonance imaging [8], it is evident that long-narrow PGSE-NMR is akin to MRI since Eq. (2) contains the full structure factor $S_0(\boldsymbol{q})$.

Variants of the long-narrow experiment have been conducted at 400 MHz proton resonance frequency on a standard Bruker Micro 2.5 imaging system. A closed-pore system was designed with about 470 aligned water-filled glass capillaries of radius $a = (10 \pm 1)\ \mu$m. MRI and standard PGSE-NMR experiments ensured that signal originated only from within the capillaries and not from the space in between them. Key parameters of the experiment are the total duration $T = 200$ ms of the gradients, the maximum gradient strength of 1.45 T/m, and the sample temperature of 40 °C. This results in $DT/a^2 = 6.4$, a factor which relates the mean squared displacement due to diffusion (D being the free diffusion coefficient of water) to the characteristic length, the pore radius a. This factor is a measure of how often molecules have traveled across the pore during application of the gradients. The experimental challenge is to make this factor sufficiently large without suffering too much signal loss due to relaxation effects. Only in this case the exponential prefactor converges sufficiently enough to the expression given by Eq. (2). Depending on the molecular mobility and the pore sizes themselves, this may require a length of the long gradient pulse of 100 ms or more.

We solved this problem primarily by replacing the long gradient pulse as shown in Fig. 1(a) with alternating gradients interspersed with a train of 180° RF pulses, spaced apart by $2\tau = 5.56$ ms, as depicted in Fig. 1(c). This results in a Carr-Purcell-Meiboom-Gill (CPMG)-like pulse sequence structure [12], for which relaxation is now controlled by T_2 rather than T_2^*. This allows the long gradient pulse to be sufficiently extended. While T_2^* is only 25 ms, T_2 is about 2 s, which enabled us to deploy a train of 36 gradient pulses in place of the continuous long gradient while preserving the NMR signal. It is important to note that these modifications do not alter the nature of the approach as suggested by Laun *et al*. [4]. It merely compensates for unavoidable imperfections of the experimental setup. While further experimental details will be published elsewhere, theoretical aspects related to this approach have been discussed in detail very recently by Laun *et al*. [13]. We further note that independent experimental results have been obtained using the unaltered long-narrow experiment in a triangular domain [14].

We have applied this adapted experiment to the bundle of 470 capillaries described above. Diffusion of the water molecules is confined in directions perpendicular to the symmetry axis of these capillaries, thus the experiment should return a structure factor corresponding to this confinement. Most notably, and unlike data obtained from single PGSE-NMR experiments to date, the real part in Fig. 2 indeed reveals a function which clearly features both positive and negative values while the imaginary part is close to zero as required for a sample with cylindrical symmetry.

Equation (2) contains both the structure factor as well as the exponential prefactor in the limit of $\delta_L \to \infty$. For a particular sample and finite δ_L, Eq. (2) needs to be modified accordingly, resulting in

$$E(q) = \exp\left\{-\frac{\gamma^2 G^2 T a^4 \xi_{-1} I_f}{D}\right\}\frac{J_1(2\pi qa)}{\pi qa} \quad (3)$$

for a cylindrical domain [13]. The second fraction in Eq. (3) holds the structure factor for cylinders oriented perpendicular to the wave vector $\boldsymbol{q}$. J_1 and a denote the cylindrical Bessel function of first order and the radius of the capillaries, respectively. The leading exponential function in Eq. (3)

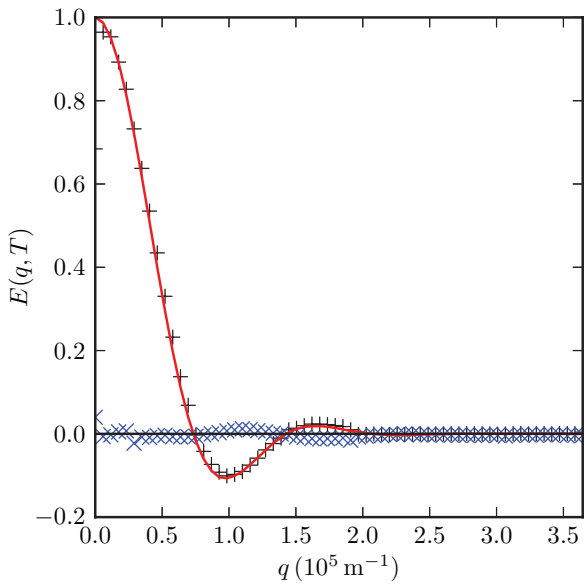

FIG. 2. (Color online) Real (+) and imaginary (×) part of the NMR signal as a function of the scattering wave vector $\boldsymbol{q}$, measured on a bundle of uniformly aligned water-filled capillaries. Note that each point represents the value at the echo maximum. The solid line represents simulated data obtained by a random walk model.

TABLE I. The first three zeros of $J_1(x)$ and the zeros of the NMR signal $E(q)$ obtained from the long-narrow and diffusion-diffractive PGSE-NMR experiments together with the derived capillary radius $a = \frac{x}{2\pi q}$.

	Zeros of $J_1(x)$	Long-narrow		PGSE-NMR	
	$x = 2\pi aq$	q (μm^{-1})	a (μm)	q (μm^{-1})	a (μm)
First	3.8317	0.075	8.1	0.066	9.2
Second	7.0156	0.146	7.6	0.117	9.5
Third	10.1735	0.197	8.2	0.170	9.5

expresses the signal attenuation, while taking into account the finite length of the long gradient. ξ_{-1} is a geometry-dependent factor which is 7/94 for the cylindrical domain, G is the time average of the long gradient amplitude, and I_f is the second moment of the normalized temporal gradient profile which is equal to 1.93 for the pulse sequence used in this work. Further details on the parameters and expressions used in Eq. (3) can be found in Laun *et al.* [13] and Grebenkov [15]. It is possible to extract the capillary radius a by fitting the real part of the NMR signal as shown in Fig. 2 to Eq. (3). We obtained $a = (8 \pm 1)$ μm, which is smaller than the actual radius. This deviation can be understood if the finite width of the narrow gradient (which in our case is composed of two gradients with an effective length of about 8 ms) is taken into account, explaining the failure to detect molecules at or near the pore wall. Instead, the center of mass position of molecules averaged over the diffusion path during the application of the narrow gradient pulse is detected which makes the pores appear to be smaller [16]. Likewise, Table I shows that zeros of the NMR signal $E(q)$ from the long long-narrow data are shifted towards higher $\boldsymbol{q}$ values compared to the zeros of the diffusive-diffractive PGSE-NMR experiment which was carried out with a narrower gradient pulse of about 2 ms. The pulse is narrower because it is not composed of two gradients which allows the center of mass to be closer to the pore wall which consistently yields a larger radius (last column in Table I). A detailed analysis of the interplay between a nonideal long and a nonideal narrow gradient pulse with respect to the obtained intensity profiles is provided by Laun *et al.* [13].

To further validate our study, we simulated the experiment with a Monte Carlo algorithm, resulting in the solid line in Fig. 2. The agreement between the simulated and NMR data is remarkable. Our method, although closely related to scattering techniques, proves to return the full structure factor. Moreover, this is achieved using a single, straightforward NMR experiment.

The measurement of a one-dimensional structure factor may be sufficient for cases in which the pores exhibit certain symmetries. However, it is desirable to extend the approach towards higher dimensions for arbitrary pore shapes. While the radon transformation or back projection can be used for image reconstruction [5,14] it comes at the cost of a large number of one-dimensional profiles needing to be taken. We therefore developed an approach which is inspired by the similarities between common MRI and the long-narrow experiment. Its two-dimensional (2D) equivalent, shown in Fig. 3, leads to an experiment which is known in conventional

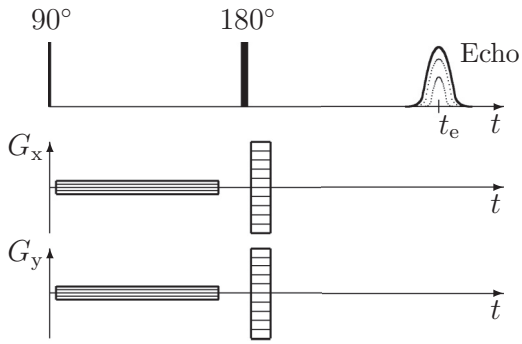

FIG. 3. 2D MRPI pulse scheme. Gradients G_x and G_y are stepped independently.

MRI as phase-encoded imaging and carries with it a convenient and unambiguous way of image reconstruction. Instead of one, now two orthogonal gradients G_x and G_y are stepped independently. The experiment retains its CPMG-like structure as for the one-dimensional case (though this is omitted in Fig. 3 for clarity) and entirely resembles a conventional 2D MRI experiment. However, there are two remarkable differences. First, the long gradients transform the experiment from one which measures displacements into one which measures positions with respect to the center of mass for each pore. Second, MRI data are acquired by sampling $\boldsymbol{k}$ space [8], while it is $\boldsymbol{q}$ space which is traversed here. Hence, we choose the name MRPI, which accounts for these differences to MRI.

We have applied a two-dimensional MRPI experiment to the aforementioned sample, thus obtaining data in which $\boldsymbol{q}$ space is traversed on a Cartesian plane in a 32 × 32 matrix. The result as shown in Fig. 4(a) is the real part of the two-dimensional structure factor which inherits its point symmetry from the object it is describing—the water confined by the capillary walls. As for the one-dimensional structure factor shown in Fig. 2, the imaginary part of the acquired signal (not shown) is close to zero in the two-dimensional data set. It is most intriguing to see in Fig. 4(b) that a simple two-dimensional Fourier transformation reconstructs the actual pore shape, averaged over all pores with an intensity profile again determined by the interplay of the nonideal gradient pulses as discussed by Laun *et al.* [13]. Remarkably, the nominal resolution of this image is 1.3 μm/pixel, however, it was achieved with moderate gradients provided by a standard microimaging system (we

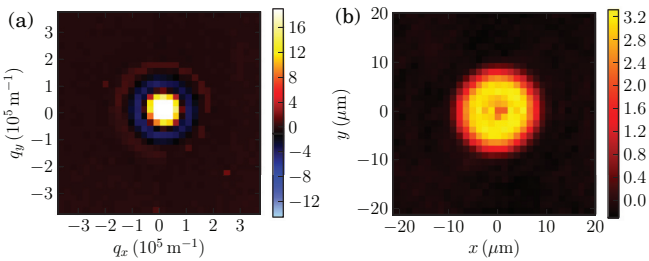

FIG. 4. (Color online) Real part of the two-dimensional structure factor as acquired with MRPI from water in a bundle of capillaries (a) and the corresponding averaged pore image obtained by a subsequent 2D Fourier transformation of these data (b).

note that the effective resolution is reduced due to diffusion during the narrow gradient pulse). Further considerations with respect to available gradient strength and the resulting applicability of the method for various pore sizes and pore fluids are discussed in Laun *et al*. [13]. Generally one needs to satisfy the condition that molecules diffuse several times across the pore while maintaining a small diffusive displacement during the narrow gradient. Despite these challenges, further development of the method and the careful choice of the pore space fluid (from gases to viscous hydrocarbons) may allow MRPI to be applied broadly. Furthermore, although the method is most promising for closed-pore systems, it may be applicable for connected pore spaces in selected cases [11].

Evidently, MRPI integrates seamlessly with proven concepts of MRI. Therefore, one may expect to find advantages and established approaches of MRI to work for MRPI as well. This may include efficient ways to sample $\boldsymbol{q}$ space by employing advanced schemes such as sparse or spiral sampling as known from conventional MRI. Furthermore, it seems possible to develop techniques similar to chemical shift imaging (CSI) [17] which may map structure factors or even averaged pore images onto low resolution images. More importantly, one does not rely on a particular symmetry or shape of the pore system. We therefore anticipate MRPI to extend the toolbox for future porous media research substantially.

We thank Professor Sir Paul T. Callaghan and Dr. Andrew Coy for useful discussions and acknowledge the Ministry of Business, Innovation & Employment of New Zealand for financial support.

[1] J. Als-Nielsen and D. McMorrow, *Elements of Modern X-Ray Physics* (Wiley, Chichester, 2011).
[2] D. Svergun, L. Fegin, and G. Taylor, *Structure Analysis by Small-Angle X-Ray and Neutron Scattering* (Plenum, New York, 1987).
[3] P. T. Callaghan, A. Coy, D. Macgowan, K. J. Packer, and F. O. Zelaya, Nature (London) **351**, 467 (1991).
[4] F. B. Laun, T. A. Kuder, W. Semmler, and B. Stieltjes, Phys. Rev. Lett. **107**, 048102 (2011).
[5] N. Shemesh, C.-F. Westin, and Y. Cohen, Phys. Rev. Lett. **108**, 058103 (2012).
[6] T. A. Kuder and F. B. Laun, Magn. Reson. Med., doi:10.1002/mrm.24515 (2012).
[7] P. C. Lauterbur, Nature (London) **242**, 190 (1973).
[8] P. T. Callaghan, *Principles of Nuclear Magnetic Resonance Microscopy* (Clarendon, Oxford, 1991).
[9] P. T. Callaghan, C. D. Eccles, and Y. Xia, J. Phys. E **21**, 820 (1988).
[10] D. G. Cory and A. N. Garroway, Magn. Reson. Med. **14**, 435 (1990).
[11] P. T. Callaghan, *Translational Dynamics & Magnetic Resonance* (Oxford University Press, Oxford, UK, 2011).
[12] S. Meiboom and D. Gill, Rev. Sci. Instrum. **29**, 688 (1958).
[13] F. B. Laun, T. A. Kuder, A. Wetscherek, B. Stieltjes, and W. Semmler, Phys. Rev. E **86**, 021906 (2012).
[14] F. B. Laun, T. A. Kuder, B. Stieltjes, and W. Semmler, http://ocs.som.surrey.ac.uk/index.php/mrpm11/index/pages/view/confschedule.
[15] D. S. Grebenkov, Rev. Mod. Phys. **79**, 1077 (2007).
[16] P. P. Mitra and B. I. Halperin, J. Magn. Reson. A **113**, 94 (1995).
[17] P. Mansfield, Magn. Reson. Med. **1**, 370 (1984).